Enhanced Thematic Mapper Plus Scan Line Corrector Geometric Processing Algorithm Theoretical Basis

Background

The Landsat 7 Enhanced Thematic Mapper Plus (ETM+) instrument achieves its 185-kilometer cross-track ground swath by using a bi-directional scan mirror to traverse the instrument line-of-sight through a 15-degree cross-track field of view. On descending passes, the mirror alternately scans west-to-east (forward scan) and then east-to-west (reverse scan). The active Earth-imaging portion of each scan lasts for, nominally, 60.743 milliseconds. During this time, the Landsat 7 spacecraft advances approximately 410 meters downtrack. If uncompensated, this spacecraft motion would add an along-track component to the scan mirror's cross-track trajectory, leading to a zig-zag scanning pattern that overlaps where one scan end adjoins the next scan start, and leaves gaps where one scan end adjoins the previous scan start. The maximum gap at the edge of the ETM+ swath is the distance traveled in two active scans plus one mirror turnaround period (11.57 milliseconds as of July 2003), less the width of one scan (480 meters). This is approximately 420 meters. The ETM+ scanning pattern without compensation for spacecraft motion, is shown in figure 1.
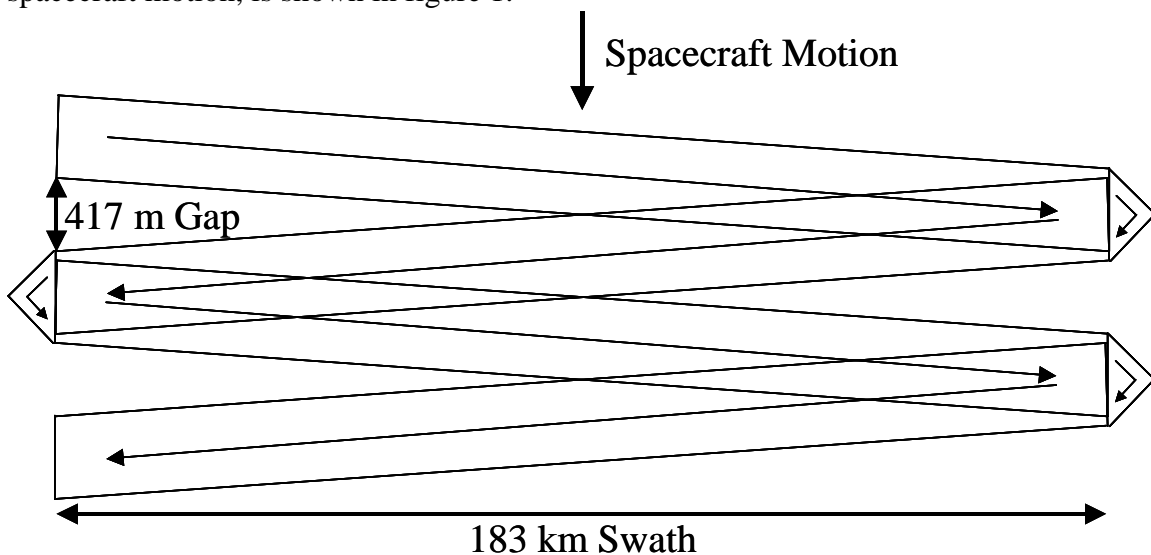

Figure 1: ETM+ Ground Scanning Pattern Without Spacecraft Motion Compensation

The ETM+ compensates for the effects of this along-track motion by using a device called the scan line corrector (SLC) [1]. The SLC uses a rotating set of parallel mirrors to displace the ETM+ line of sight in the fore-to-aft direction during the active scan, at a constant rate designed to counteract the spacecraft motion. The SLC retraces, moving from its end-of-scan full aft position to its scan-start full forward position, during the turnaround time while the scan mirror is changing directions. The SLC adjusts the ETM+ along-track pointing so that, if the scan mirror were not moving, it would view a constant location during each active scan period. This along-track "staring" makes the scan mirror's cross-track scans nearly perpendicular to the spacecraft ground track, minimizing end-of-scan overlap and gaps. The resulting scanning pattern is shown in figure 2.
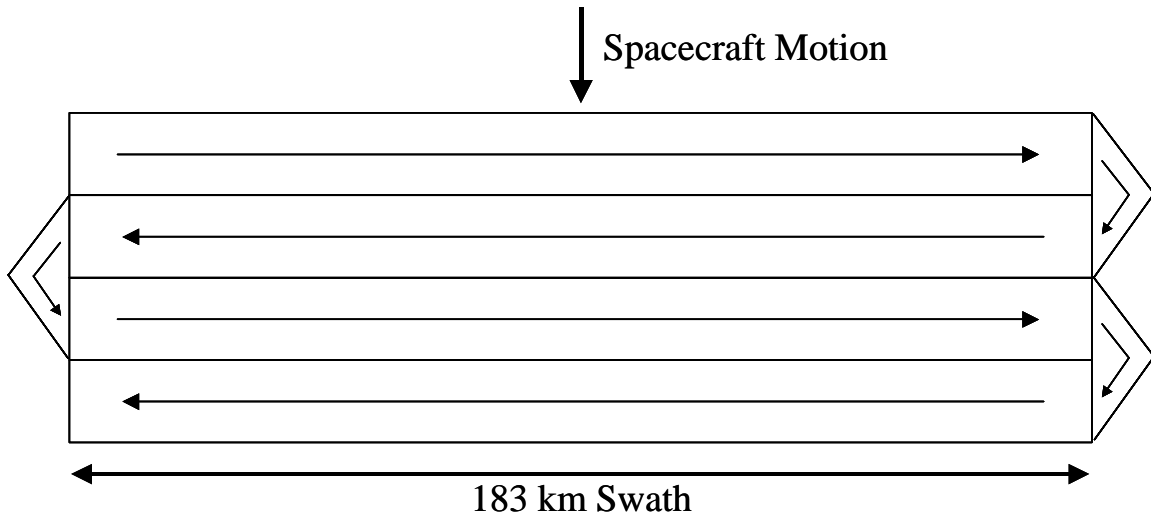
Figure 2: ETM+ Ground Scanning Pattern With Scan Line Corrector Compensation

Normal ETM+ SLC motion halted at approximately 21:44:07 UTC on May 31, 2003. This anomaly manifested itself in the ETM+ image data as duplicate imagery in alternate pairs of adjacent scans, at the edges of the Landsat 7 swath. This scan overlap, and the less obvious intervening scan-to-scan gap, is a result of the loss of forward motion compensation provided by the SLC. On June 6, 2003, after the failure was isolated and traced to the SLC, the mechanism was commanded off. With the exception of a brief test on September 7, 2003, the SLC has remained off since that time. An example of the SLC-off imagery, processed to Level 0R, is shown in figure 3. This figure shows a full resolution window extracted from the left (western) edge of a scene. Note the presence of a calibration shutter incursion at the end of each reverse scan.
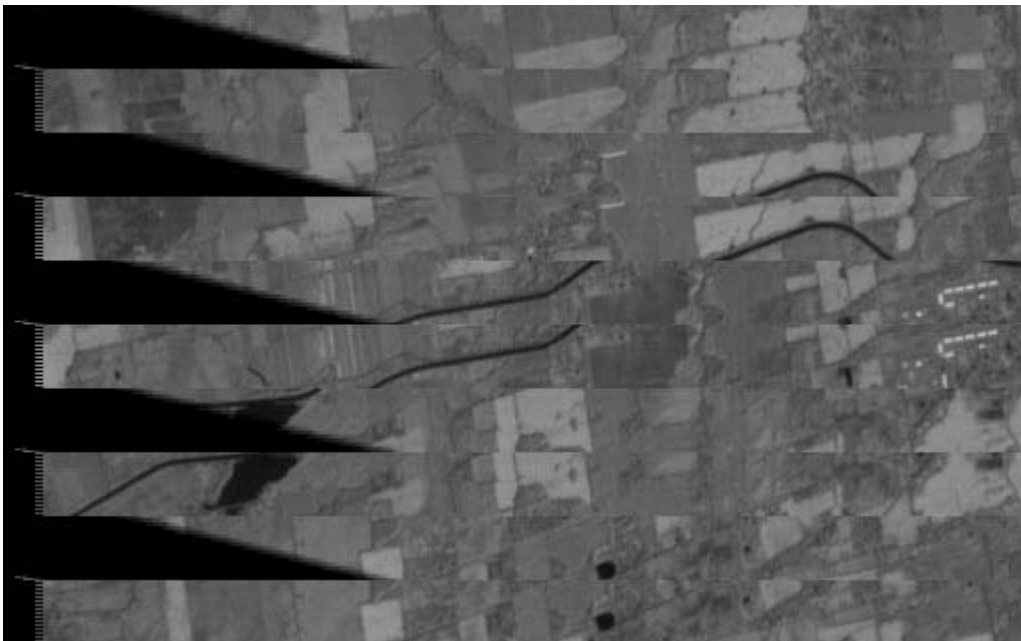

Figure 3: SLC-Off Level 0R Image Window (Band 8)

Although a redundant copy of the SLC mechanism itself was not provided in the ETM+, the control electronics are duplicated. Although analysis of the post-anomaly image and telemetry data indicated a mechanical failure, a test of the redundant SLC electronics was conducted on September 7, 2003. This test yielded results nearly identical to those observed using the primary electronics, confirming that the anomaly is due to a mechanical failure of the SLC. Given the failure to recover proper SLC function using the redundant electronics, henceforth the normal ETM+ operating mode will be SLC off. The changes to the ETM+ geometric correction algorithms, required to successfully process SLC off data, are described in the following sections.

Scan Line Corrector Geometric Model
The operating state of the scan line corrector is identified in the spacecraft telemetry in serial word G of the payload correction data (PCD) [2]. Bits 0 and 1 of serial word G indicate whether the primary (SLC1), or redundant (SLC2) control electronics are being used to drive the SLC. The PCD serial word bit settings for the SLC operating mode are summarized in table 1.

SLC State	Serial Word	Bit	Setting	SLC Mode
SLC Off	G	0	0	0
	G	1	0	
SLC1 On	G	0	1	1
	G	1	0	
SLC2 On	G	0	0	2
	G	1	1	
Invalid SLC State	G	0	1	-
	G	1	1	

Table 1: SLC Mode PCD Serial Word Settings

The SLC is modeled using a linear fore-to-aft motion with adjustments for repeatable nonlinear behavior [3]. Two fifth-order polynomials, similar to those used to model the ETM+ scan mirror non-linearity, are used to model the repeatable along-track deviations from linearity of the SLC when operating with the primary and redundant electronics. Since SLC motion is in the same direction for each scan, separate correction polynomials for each scan direction are not required. In fact, since prelaunch characterization data quantifying the non-linear behavior of the SLC was unavailable, these SLC correction polynomials have been set to zero since launch with the actual SLC non-linear motion being absorbed into the scan mirror across-scan profiles in the course of the on-orbit scan mirror calibration process.

The Landsat 7 Calibration Parameter File (CPF) SCAN_LINE_CORRECTOR group contains the parameters used to characterize the SLC's motion. These parameters are listed in table 2. As noted above, the fifth-order polynomial coefficients have all been zero since launch. The collection of data with the SLC off has made it possible, in principle, to separate the effects of SLC non-linearity from scan mirror non-linearity, but, since this would only be useful for pre-anomaly data which is already well characterized and calibrated, an update to the SLC fifth-order polynomial coefficients is not planned.

Parameter	Description	CPF Name
$SLCa_{j=0,5}$	Primary SLC fifth-order polynomial coefficients	Primary_Corrector_Motion
$SLCb_{j=0,5}$	Redundant SLC fifth-order polynomial coefficients	Secondary_Corrector_Motion
$SRate_A$	Primary SLC scan rate => Positive = fore-to-aft	Primary_Angular_Velocity
$SRate_B$	Redundant SLC scan rate => Positive = fore-to-aft	Secondary_Angular_Velocity
θ_{rest}	Pointing angle of the SLC at its rest (unpowered) position => Positive = aft	Unpowered_Pointing_Bias

Table 2: SLC Calibration Parameters

One of the items listed in table 2 has been added to the SLC parameter group CPF as a result of the SLC failure. The origin for the determination of viewing angles in the ETM+ coordinate system is the pointing direction corresponding to the center of the ETM+ focal plane when the scan mirror is at its mid-scan position [4]. The reference, or "zero", cross-track viewing angle is therefore established by the orientation of the SLC at the mid-scan time. This may not exactly coincide with the SLC's natural rest position. When unpowered the SLC returns to this rest position, so the Unpowered_Pointing_Bias parameter was added to the CPF to capture the difference between the SLC's powered mid-scan position and its rest position. This parameter is used in the SLC-off geometric correction algorithm to remove the small pointing bias that would result if the unpowered SLC was assumed to be oriented at its zero, or powered mid-scan, position.

In the Landsat 7 ETM+ geometric model, the SLC contributes only to the across-scan viewing angle computations [4]. The SLC effects are added to the contributions due to the cross-scan scan mirror non-linearity, the cross-scan band offset, and the cross-scan component of the detector location, to compute the net cross-scan pointing angle for a given ETM+ detector. The SLC effects consist of two parts: the linear fore-to-aft motion and the repeatable non-linear behavior captured by the fifth-order polynomial. The linear motion is modeled using the initial scan start fore-pointing angle and the total SLC travel angle. These SLC parameters are listed in table 3. Note that these parameters and the way they are used to compute cross-scan viewing angles is the same for all SLC modes. The SLC mode determines how the SLC calibration parameters are used to populate the SLC model parameters.

Parameter	Description
fore_angle	The SLC pointing angle at scan start
slc_angle	The total SLC travel angle for one scan
$c_{j=0,5}$	SLC non-linearity fifth-order polynomial coefficients

Table 3: SLC Model Parameters

These parameters are computed from the SLC calibration parameters listed in table 2, and the active scan time (also provided in the Landsat 7 CPF), as a function of the SLC mode, shown in table 1, as follows:

        Case 0: (SLC mode = 0)   Unpowered SLC
            fore_angle = $-\theta_{rest}$
            slc_angle = 0
            $c_j = 0$ for j=0..5

Case 1: (SLC mode = 1)   Primary SLC
    fore_angle = $SRate_A$ * Active Scan Time / 2
    slc_angle = $SRate_A$ * Active Scan Time
    c_j = $SLCa_j$ for j=0..5

Case 2: (SLC mode = 2)   Redundant SLC
    fore_angle = $SRate_B$ * Active Scan Time / 2
    slc_angle = $SRate_B$ * Active Scan Time
    c_j = $SLCb_j$ for j=0..5

An SLC mode of 3 represents an invalid SLC state and should be reported as an error if detected. Note the minus sign in front of θ_{rest} in the SLC mode 0 case. The SLC calibration parameter sign convention is such that a positive SLC rate represents fore-to-aft motion and a positive pointing bias represents an aft pointing bias. The sign convention used in the computation of sensor viewing angles treats forward pointing angles as positive and aft pointing angles as negative, requiring a reversal of the pointing bias sign. This is also reflected in the computation of the SLC angle, in which the linear SLC rate has a negative sign. For a given time from scan start (T), the model parameters are used to compute the linear and non-linear SLC contributions as:

slc_linear = fore_angle - slc_angle * T / Active Scan Time
slc_nonlin = $c_0 + (c_1 * T) + (c_2 * T^2) + (c_3 * T^3) + (c_4 * T^4) + (c_5 * T^5)$

In the EROS Data Center implementation the "Active Scan Time" used to compute slc_linear is the actual time for the current scan although it would be more theoretically correct to use the nominal value used to compute slc_angle.

These contributions are added to the scan mirror, band, and detector effects, as described in reference 4, to compute the net cross-scan viewing angle:

cross-scan angle = slc_linear + 2*(slc_nonlin + cross-scan mirror non-linearity)
                        + cross-scan band offset + cross-scan detector angle

The non-linearity terms are doubled to be consistent with the treatment of these deviations as mirror angles, which are doubled when the line-of-sight is reflected off the mirror, in the along-scan equations. This has no practical effect on the SLC since, as noted above, the SLC non-linearity parameters have been set to zero since launch.

Scan Gap Resampling Algorithm
The primary resampling challenge posed by the SLC-off data is the need to gracefully handle the large asymmetrical scan gaps caused by the uncompensated forward motion of the Landsat 7 spacecraft during the ETM+ active scan time. Although normal ETM+ imagery contains scan gaps that vary in size with latitude and scan mirror turnaround time/bumper wear, these gaps are typically small, no more than 1 or 2 pixels, and relatively uniform along-scan. The gaps induced in the SLC-off data vary in width from

approximately 13-14 multispectral pixels where the beginning of one scan abuts the end of the following scan, to near zero at mid-scan, to an overlap of nearly 13 multispectral pixels where the end of one scan abuts the beginning of the following scan. This dramatic along-scan change in the gap size is as much a problem as the large magnitude of the worst-case gap. The gap asymmetry requires the interpolation logic to be flexible enough to adjust its behavior to the local scan gap rather than treating the gap uniformly across the scan. The magnitude of the gap at the scene edge raises the question of whether all gap pixels should be interpolated.

To see why gap asymmetry is a problem it is helpful to understand how the resampling software implemented in the Landsat 7 Image Assessment System (IAS) and Level 1 Product Generation System (LPGS) handles the scan gap. Details of the gap algorithm are provided in reference 4. For nearest neighbor (NN) resampling the gap is only a slightly more complicated case of the normal algorithm in which, for each output point, the closest input detector sample must be identified and selected as the output image value. This logic is not particularly sensitive to the size or shape of the scan gap, but it does produce odd-looking artifacts if the gap becomes too large. When this happens the NN logic will "smear" the imagery from the active scans into the gap, leaving a discontinuous boundary at the gap midpoint where the closest-scan transition occurs. An example of this effect is shown in figure 4.
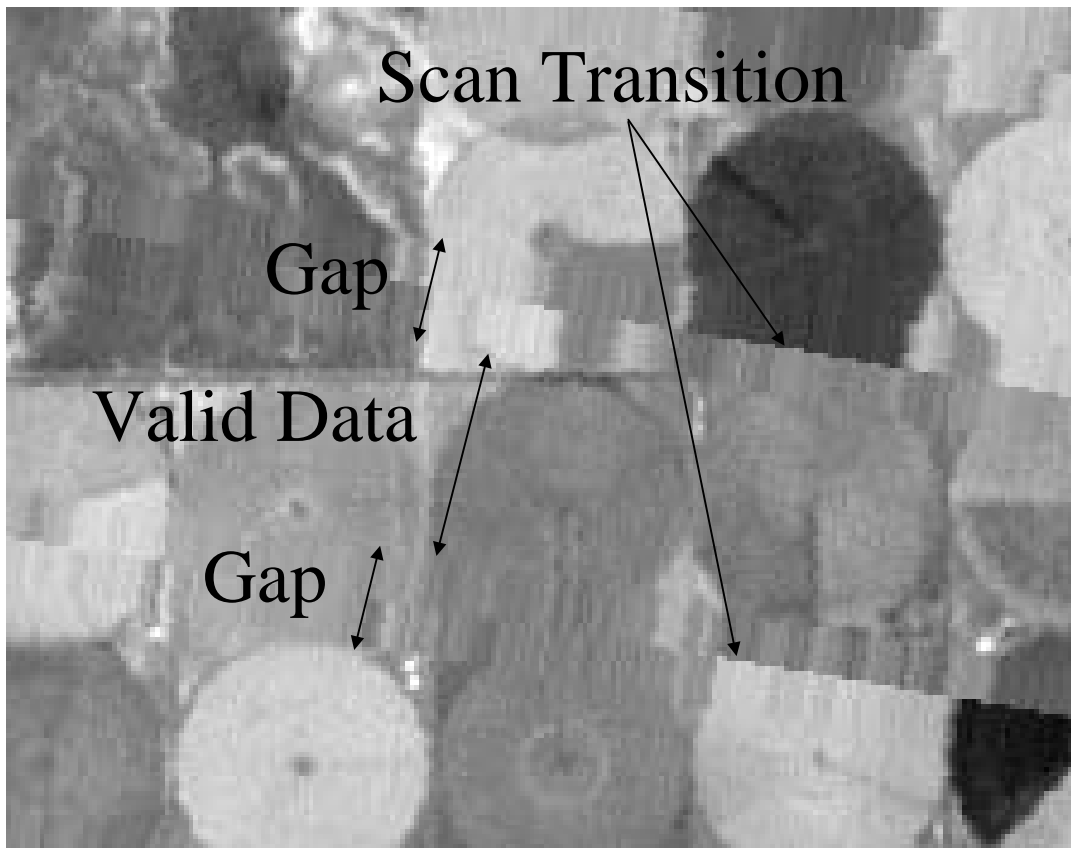

Figure 4: Example of NN Gap Fill

Suppressing this artifact requires gap interpolation control logic. The IAS/LPGS implementation was modified to perform scan gap computations for each output image point that falls between ETM+ scans. For each gap point the distance to the closest scan (measured pixel center to pixel center) and the total scan gap width are calculated using the resampling grid. These distances are compared to a user-provided gap threshold (MAX_GAP) to determine whether the point lies within MAX_GAP/2 of the closest scan or if the total scan gap at the point is less than MAX_GAP+1. If so, the point is populated with the value of the nearest detector. If not, the point is populated with a fill value. This results in a scan gap interpolation pattern that replicates the data at the edges of the scan gap out to MAX_GAP/2 for the entire gap area and populates all gap pixels where the scan edge to scan edge distance is less than MAX_GAP. The geometry of the minimum distance and total gap threshold distances is shown in figure 5.
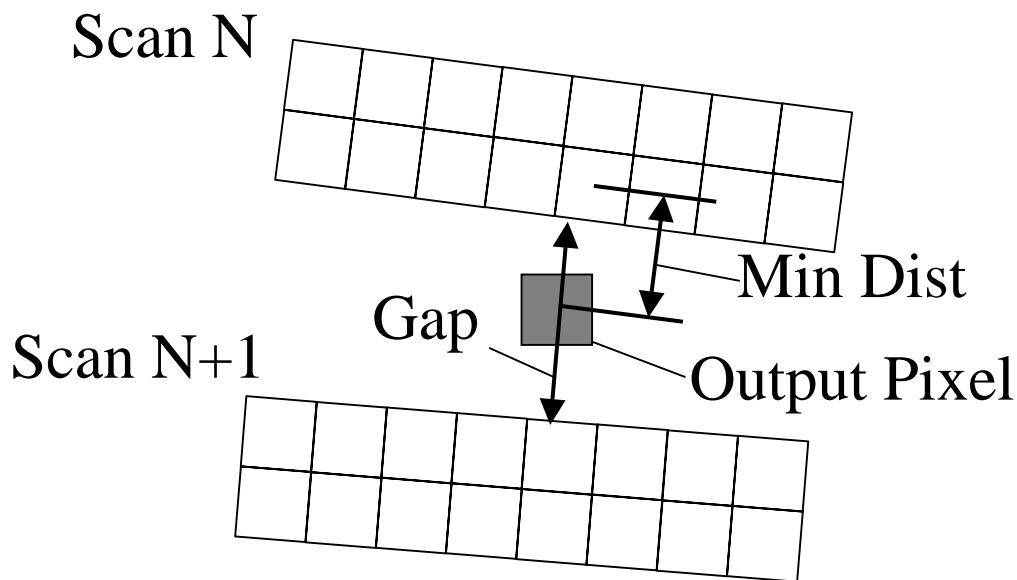

Figure 5: Edge-to-Edge Gap and Center-to-Center Distance Thresholds

For the cubic convolution (CC) and modulation transfer function compensation (MTFC) interpolative resampling kernels the situation is more complicated. These kernels require four evenly spaced input lines of data to construct an output image value. The IAS/LPGS gap resampling logic meets this requirement by "extending" the ETM+ scans with synthetic detector image lines that completely cover the gap. The extended lines are constructed by a preprocessing step that uses one-dimensional CC interpolation to first align the samples in the next (lower) scan with the samples in the current (upper) scan, and then uses one dimensional cubic spline interpolation to construct evenly spaced image lines spanning the gap, from the aligned samples from the upper and lower scans. The resulting extended scans provide complete coverage of the output image area with suitable overlap to allow the 4-by-4 (actually 4-by-6 to allow for detector-specific delay offsets) interpolation kernels to operate normally for all output pixels. This two-pass gap interpolation approach works well for the small, uniform gaps found in normal ETM+ imagery. The basic extended scan algorithm is described in reference 4.

In principle, a large scan gap poses no insurmountable challenge to this gap interpolation approach. As long as all of the data needed to construct the extended scan lines are available from the lower scan, the spline interpolation can proceed as normal. Problems arise when the asymmetry in the gap causes the number of extended lines required to cover the underlap portion of the gap to extend beyond the lower edge of the following scan in the overlap area. With a 13 pixel maximum gap the resampler will require at least 15 extended lines (two extras to overlap the top edge of the neighboring scan). Where the adjacent scans overlap by 13 lines, this 15-line buffer will extend below the lower edge of the adjacent scan. The extended scan logic will fail in this situation unless it can accommodate a variable number of extended lines within one scan. The IAS/LPGS logic was modified to test for the overlap case and insert fill into the extended scan data if the extended lines fall more than six lines into the adjacent scan. Six lines provide sufficient overlap for complete gap coverage while limiting the amount of duplicate data in adjacent extended scans, and avoiding the "extended scan overshoot" problem described above. Gap interpolation approaches that operate directly on the adjacent scan data without constructing an extended scan may be more easily adapted to this asymmetrical gap situation.

The CC (and MTFC) gap interpolation control logic differs from the NN method in that it uses only the total gap width criterion to decide whether or not to interpolate a value for a gap pixel. The need for data from both the scan above and the scan below to interpolate gap pixel values makes it undesirable to generate output values for any gap pixels when the gap size becomes too large. This makes the CC gap fill pattern exhibit a more abrupt transition from total gap interpolation to no gap interpolation than is the case with NN resampling. This is depicted graphically in figure 6. An example of corresponding band 8 image windows processed with NN and CC interpolation, is shown in figure 7.
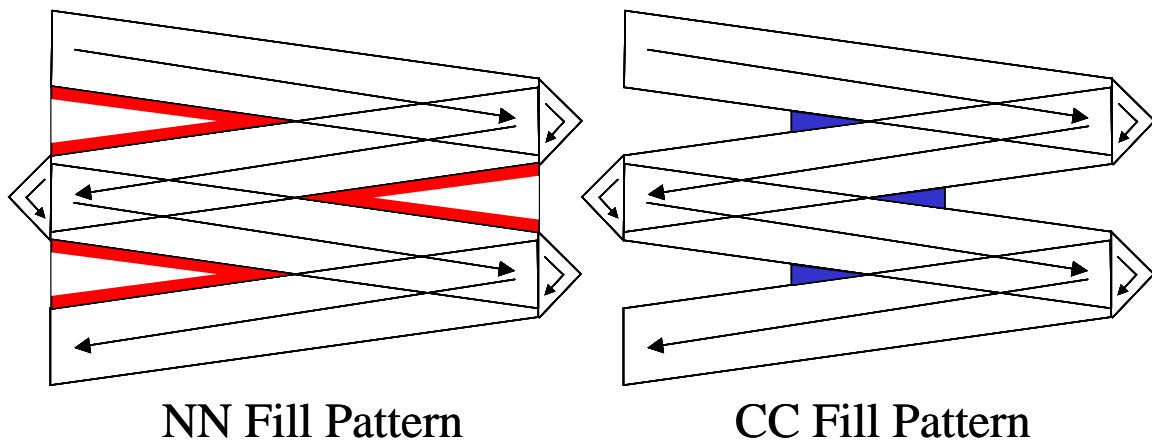

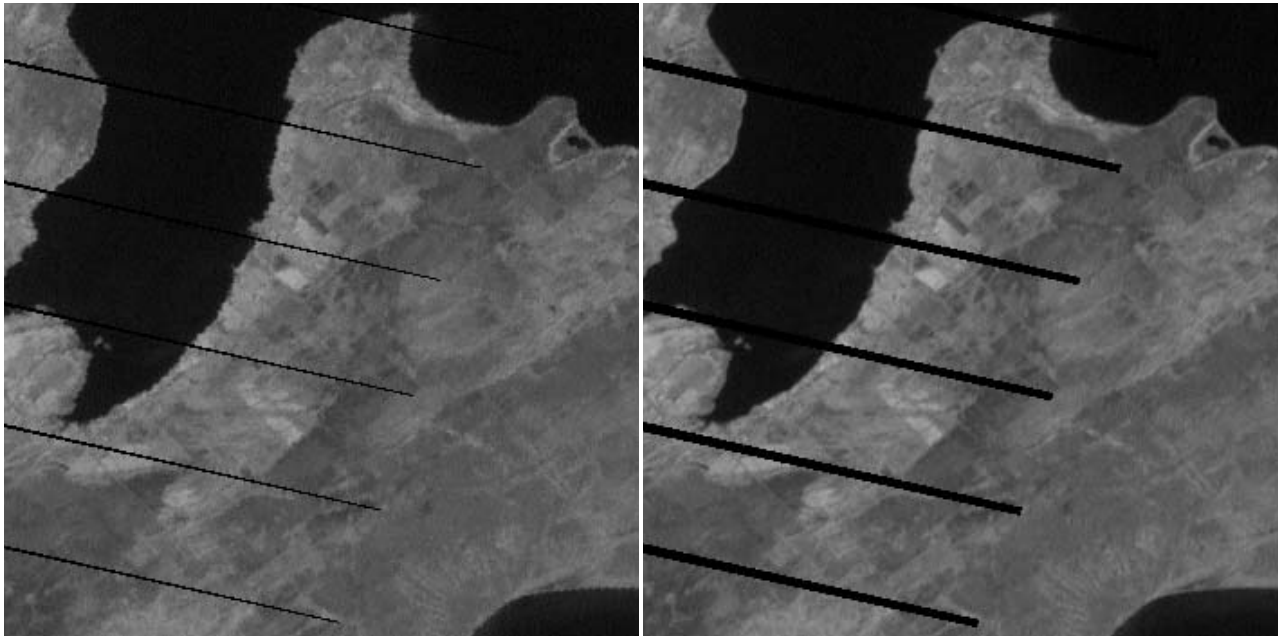Figure 6: NN versus CC/MTFC Fill Patterns

Figure 7: NN (left) and CC (right) Gap Fill Example

There are thus two significant changes to the image resampling logic required to properly support Level 1G product generation from SLC-off data. The first is the need for improved gap pixel interpolation control to prevent image smearing and the second is enhanced extended scan processing that can accommodate large asymmetric scan gaps. The ways in which the IAS/LPGS resampling software was modified to address these problems has been noted above. Other implementations that employ alternative approaches to scan gap interpolation may require slightly different adjustments.

Shutter Incursion Suppression Algorithm
One final (optional) refinement to the image resampling procedure, motivated by the lack of SLC motion, is to use the overlapping imagery at the edges of the scene to suppress the calibration shutter incursions present at the end of reverse scans. These incursions are evident in figure 3 above. Since the data from the beginning of the following forward scan largely overlaps the end of each reverse scan, it is possible to favor the data from the forward scans in these areas to minimize the impact of the shutter data on the resampled image.

To avoid the calibration shutter incursion data it is first necessary to identify the data regions affected by these incursions. This is done by estimating the size of the shutter incursion for each scene using the average scan mirror turnaround time, computed from the mirror scan correction data for that scene. Reverse scan pixels determined to be subject to the shutter incursion, based upon this computation, can then be avoided in preference to overlapping pixels from the beginning of the adjacent forward scan.

The algorithm for estimating the size of the reverse scan shutter incursion has the following inputs:

    1. Band number
    2. Calibration parameter file
    3. Mirror scan correction data
    4. Three new constants:
        a. ideal_turnaround_time_ms = 10.6 milliseconds => ideal turnaround time
        b. ideal_turnaround_offset_minor_frames = 4.503 minor frames => ideal TAT offset at edge of image
        c. shutter_slope = 0.7548 => shutter slope across focal plane

The number of reverse scan pixels affected by the shutter incursion is estimated as follows:

1. Define a variable called band_offset_pixels to contain the value from the CPF Reverse_Odd_Detector_Shift array for that band:

  band_offset_pixels =
    CPF.Focal_Plane_Parameters.Odd_Even_Offsets.Reverse_Odd_Detector_Shift[band];

2. Convert ideal_turnaround_offset_minor_frames to pixels by multiplying by 2, for band 8, multiplying by 1 for bands 1-5, and 7, and by dividing by 2, for band 6:

```
   if ( band = 8 )
       ideal_turnaround_offset_pixels = ideal_turnaround_offset_minor_frames * 2
   else if ( band = 6 )
       ideal_turnaround_offset_pixels = ideal_turnaround_offset_minor_frames / 2
   else
       ideal_turnaround_offset_pixels = ideal_turnaround_offset_minor_frames
```

3. Compute the scene average total scan time from the MSCD as follows:
  Mean_Total_Scan_Time = (MSCD[NScans-1].ScanTime - MSCD[0].ScanTime)
                    / (NScans-1) in seconds
Multiply the result by 1000 to convert to milliseconds.

4. Compute the scene average turnaround time, in milliseconds, by subtracting the nominal active scan time (scaled to milliseconds) from the CPF:
  TAT = Mean_Total_Scan_Time - CPF.Scanner_Parameters.Active_Scan_Time/1000
Note: The Active_Scan_Time is provided in units of microseconds in the CPF.

5. Compute the band-dependent sensor dwell (sample) time in milliseconds:
    if (band = 8) dwell_time_ms = CPF.Scanner_Parameters.Dwell_Time_15/1000
    else if (band = 6) dwell_time_ms = CPF.Scanner_Parameters.Dwell_Time_60/1000
    else dwell_time_ms = CPF.Scanner_Parameters.Dwell_Time_30/1000
Note: The Dwell_Time_NN parameters are provided in units of microseconds in the CPF.

6. Compute the expected shutter incursion, incursion_pixels, for this band using the 3 newly defined constants and the dwell time as follows:
  incursion_pixels = (TAT - ideal_turnaround_time_ms) / dwell_time_ms
                + ideal_turnaround_offset_pixels + shutter_slope*band_offset_pixels

7. Round incursion_pixels up to the next highest multiple of 5 pixels to provide a margin.

In the scan overlap areas within incursion_pixels of the end of a reverse scan, output pixels that are covered by the following forward scan, use the forward scan data to interpolate the output pixel value.

Summary
The changes required to accommodate SLC-off data in the ETM+ geometric model are trivial, involving only testing the appropriate telemetry serial words from the PCD to detect this condition, and then replacing the normal time-dependent SLC motion with a fixed pointing offset provided in the CPF. The impacts on the image resampling algorithms are more complex and implementation dependent. The large, asymmetrical scan-to-scan gaps caused by the lack of SLC motion can create performance issues for the scan gap interpolation algorithm. The adjustments made to the USGS Level 1 Product Generation System resampling logic have been described to provide an example of how these issues can be addressed. Other implementations of the gap resampling procedure may require somewhat different, or no, modifications.

References
1. Landsat 7 Science Data Users Handbook, http://ltpwww.gsfc.nasa.gov/IAS/handbook/handbook_toc.html, NASA Goddard Space Flight Center Landsat Project Science Office, Greenbelt, Maryland, August 2003.

2. Landsat 7 System Data Format Control Book (DFCB) Volume IV – Wideband Data. Revision L, document number 23007702-IV-L, Lockheed Martin Missiles and Space, Philadelphia, Pennsylvania, June 1999.

3. Landsat 7 System Calibration Parameter File Definition. Revision 3, document number 430-15-01-002-3, NASA Goddard Space Flight Center, Greenbelt, Maryland, April 1999.

4. Landsat 7 Image Assessment System (IAS) Geometric Algorithm Theoretical Basis Document, Version 3.2, U.S. Geological Survey EROS Data Center, Sioux Falls, South Dakota, July 1998.